Eur. Phys. J. B **9**, 525–532 (1999)

THE EUROPEAN PHYSICAL JOURNAL B

EDP Sciences

Harmonics generation and chaos in scattering of phonons from anharmonic surfaces

P. Zieliński[a], Z. Łodziana, and T. Srokowski

Institute of Nuclear Physics, ul. Radzikowskiego 152, 31-342 Kraków, Poland

Received 9 November 1998

Abstract. The effective equations of motion for a surface atom in an anharmonic surface potential have been derived for dispersionless one-dimensional substrates. The system is equivalent to a non-linear damped oscillator (Duffing oscillator) with the forcing term depending on the form of the incident wave. Efficiency of harmonics generation, phonon reflection coefficients, effective local density of states, regions of chaotic motion and windows of periodic motion have been comparatively evaluated for the system subject to an oscillating external force and to the irradiation by a monochromatic phonon coming from the bulk. Comparison of the resonant desorption of the surface atom within a given time interval has been made for the same example of anharmonic surface potential in both types of perturbation.

PACS. 68.35.Ja Surface and interface dynamics and vibrations – 65.50.+m Thermodynamic properties and entropy – 79.70.+q Field emission, ionization, evaporation, and desorption

1 Introduction

Anharmonicity is ubiquitous in the dynamics of the crystal surfaces even though the atomic motions in the bulk crystal might be satisfactorily described within harmonic approximation. The reasons for that lie in a lower coordination of the surface atoms and in their exposition to external influences [1]. Both of these factors contribute to the enhancement of the vibrational amplitudes of the surface atoms and may result in such strongly anharmonic effects as structural instabilities, *e.g.* surface reconstruction phase transitions [2], or the complete desorption of the atoms from the surface [3].

It is, therefore, plausible to assume, at least in a first approximation, that the anharmonicity is concentrated close to the surface only, whereas the bulk crystal remains perfectly harmonic. This approach allows one to reduce the number of the degrees of freedom involved in the corresponding effective equations of motion to those that explicitly participate in the anharmonic interactions [4]. The effective equations of motion then are generally Volterra Integro-Differential Equations (VIDE) [1,4]. The remaining or "harmonic" degrees of freedom contribute to the corresponding memory kernels. In the particular case of dispersionless bulk crystals the memory kernels take on a delta-like form so that the corresponding effective equations of motion reduce to just differential equations.

In the present paper we consider the dynamics of an anharmonic surface in a one-dimensional dispersionless harmonic crystal. We show that when such a system is subject to an external force applied to the surface atom, its effective equation of motion is equivalent to that of an anharmonic damped oscillator or, in the special case of the surface potential given by a polynomial, to the Duffing oscillator [5]. The equation of motion for the same system irradiated by a phonon coming from the bulk can be also expressed in this form with, however, the forcing term dependent on the incident wave.

Section 2 contains a simple derivation of the above effective equations of motion and gives their explicit form for monochromatic incident phonons. Conditions for homoclinic instability in the specific limit of a very light or very stiff substrate are also given in Section 2. Examples of numerical results for an analogue of the local density of states, here called energy loss coefficient, for efficiencies of harmonics and subharmonics generation and for phonon reflection coefficients in the ranges of regular and chaotic solutions are presented in Section 3. The numerical analyses do not require any restrictions on the model parameters. The parameters used in Section 3 are chosen so as to enable a direct comparison of the solution of the new differential equation for the phonon scattering with the known behaviour of the Duffing oscillator. In Section 4 the problem of escape of the surface atom from its initial equilibrium position, relevant in the study of desorption, is numerically solved for both types of equations.

2 Equation of motion for a surface atom on a dispersionless substrate

To model the surface anharmonicity we assume that the surface atom of mass M, while interacting with the bulk

[a] e-mail: zielinsk@alf.ifj.edu.pl

in a harmonic way, is additionally placed in a local anharmonic potential $V(u(t))$, where $u(t)$ stands for the time-dependent one-dimensional displacement of the surface atom from its initial position. The local potential breaks the translational invariance of the system and has a physical meaning of a heavy motionless anvil or support the surface is attached to.

In the long wavelength limit the bulk crystal is approximated by a continuous medium. In the simplest one-dimensional case the medium reduces to a semi-infinite elastic string extended in the range $x = 0 \ldots \infty$. The initial position of the surface atom corresponds to $x = 0$. Denoting by $u(x,t)$ the displacement of the element of the string at the point x as a function of time t one gets the following equations of motion for the described system under an external force $f_0(t)$ applied to the surface atom:

$$\frac{\partial^2 u(x,t)}{\partial t^2} = c^2 \frac{\partial^2 u(x,t)}{\partial x^2}, \quad \text{for } x > 0, \tag{1a}$$

$$\frac{\partial^2 u(0,t)}{\partial t^2} = \frac{1}{M}\left(-\frac{\partial V(u(0,t))}{\partial u(0,t)} + T\left.\frac{\partial u(x,t)}{\partial x}\right|_{x=0} + f_0(t)\right), \quad \text{for } x = 0. \tag{1b}$$

Here $c = \sqrt{T/\rho}$ is the sound velocity in the string, T is the stiffness coefficient and ρ is the linear density of the string.

Since the string is dispersionless, every wave of whatever form propagates in it without changing its form, so that every solution of the equation (1a) can be written as a sum of two waves: one travelling to the right $u(t,x) = u(\zeta_-)$ with $\zeta_- = ct - x$ and the other travelling to the left $u(t,x) = u(\zeta_+)$ with $\zeta_+ = ct + x$ [6]. Because our string is semi-infinite and the force $f_0(t)$ is applied to its left end, the only existing solution is an outgoing wave $u(t,x) = u(\zeta_-)$. Equation (1a) then is satisfied everywhere, whereas the limit condition (Eq. (1b)) for $x = 0$ transforms into the following ordinary differential equation:

$$M\frac{\partial^2 u(t)}{\partial t^2} + \frac{T}{c}\frac{\partial u(t)}{\partial t} + \left.\frac{\partial V(u)}{\partial u}\right|_{u=u(t)} = f_0(t). \tag{2}$$

The latter equation describes a damped forced anharmonic oscillator or, in the case of the potential $V(u)$ given by a polynomial, Duffing's oscillator [5] with the damping constant $\Gamma = T/c$. The role of the harmonic degrees of freedom is now reduced to an effective damping.

The same reasoning can be adopted to derive the equation of motion for the surface atom under an incident wave coming from the bulk. Then the solution will be the sum of the incident wave $u_i(x,t) = u_i(\zeta_+) = u_i(ct + x)$ and of an outgoing or reflected wave $u_r(t,x) = u_r(\zeta_-)$. As before equation (1a) is satisfied for both waves, whereas equation (1b) takes on the following form:

$$M\frac{\partial^2 (u_r(0,t) + u_i(0,t))}{\partial t^2} + \frac{T}{c}\frac{\partial (u_r(0,t) - u_i(0,t))}{\partial t} + \left.\frac{\partial V(\nu)}{\partial(\nu)}\right|_{\nu = u_r(0,t)+u_i(0,t)} = 0, \tag{3a}$$

or with the substitution $u_i(0,t) + u_r(0,t) = u(t)$

$$M\frac{\partial^2 u(t)}{\partial t^2} + \frac{T}{c}\frac{\partial u(t)}{\partial t} + \left.\frac{\partial V(u)}{\partial u}\right|_{u=u(t)} = \frac{2T}{c}\frac{\partial u_i(t)}{\partial t}\,. \tag{3b}$$

Here again one ends up with an ordinary differential equation with either the unknown function $u_r(0,t)$, describing the reflected wave or, equivalently with the unknown function $u(t)$ corresponding to the total effective displacement of the surface atom. The most common form of the incident wave is a monochromatic phonon

$$\begin{aligned} &u_i(ct + x) = a \sin\left[\frac{\omega}{c}(ct + x) + \varphi\right], \quad ct + x \geq 0; \\ &u_i(ct + x) = 0, \qquad\qquad\qquad\qquad\quad ct + x < 0. \end{aligned} \tag{4}$$

The solution of the analogous problem with a harmonic potential can be easily found with the use of the Fourier transform for each frequency ω separately [7]. The present nonlinear equation must, however, be solved numerically unless restrictive approximations are made. Linearisation or limitation to a few harmonics [8] preclude *e.g.* any instance of chaos, which is *a priori* to be expected for certain ranges of the model parameters. To enable any numerical treatment, the actual form of the wave front should be defined. The condition of the wave vanishing for $ct + x < 0$ in equation (4) is the simplest choice implying an abrupt switching on of the perturbation.

To make the comparison of the equations (3a) and (3b) with the well known Duffing oscillator [5,9] easier we shall consider here a polynomial form of the local potential

$$V(u) = \frac{1}{2}Au^2 + \frac{1}{3}Cu^3 + \frac{1}{4}Bu^4. \tag{5}$$

The proper choice of the coefficients A, C and B allows one to model a double-well potential corresponding to the surface atom participating in a surface reconstruction phase transition [2] as well as some approximate potentials useful in the discussion of the desorption [1,3].

With the incident wave of equation (4) and with the local potential of equation (5) the explicit differential equation for the unknown co-ordinate $u(t)$ of the surface atom and, at the same time, for the reflected wave $u_r(\zeta)$, reads

$$M\frac{\partial^2 u}{\partial t^2} + \frac{T}{c}\frac{\partial u}{\partial t} + Au + Cu^2 + Bu^3 = 2\omega\frac{T}{c}a\cos(\omega t + \varphi). \tag{6}$$

Solutions of the equations (2) and (3) provide the time-dependent response of the surface atom subject to an external force and to the irradiation by a phonon coming

from the bulk respectively. Once the corresponding solutions are known the quantitative estimates of experimental observables can be computed.

The systems described by equations (2) and (3) are non integrable and show irregular or chaotic behaviour at least in certain ranges of their parameters. As a signature of the fully developed chaos we use, throughout this paper, the positive value of the Lyapunov exponent. Before showing such results for arbitrary values of the model parameters we present here estimates for so called homoclinic instabilities [10] in the specific limit of a weak f_0, (or a) and $\Gamma = T/c$ which quantities are treated as small in the first order perturbation theory. To reveal the difference between equation (2) for an external force and equations (3) for the phonon scattering in this limit we put the same values $A = -1$, $B = 1$, $C = 0$, $M = 1$ in both cases and study the forcing terms $f_0(t) = f_0 \cos(\omega t)$ and $u_i(x,t) = a \sin(\omega t + x\omega/c)$ respectively. The application of the Melnikov method [11] provides the following threshold condition for the onset of the homoclinic instability in equation (2)

$$\Gamma < \left(3\sqrt{2}/4\right) f_0 \pi\omega \text{ sech } (\pi\omega/2). \tag{7}$$

Accordingly, the homoclinic instability occurs in the region of frequency ω in which the function ω sech$(\pi\omega/2)$ is big enough. The region is the larger the stronger is the amplitude of the applied force f_0 with respect to the effective damping constant Γ. The condition for the homoclinic instability in the case of phonon scattering (Eq. (6)) obtained in the same way is

$$1 < \left(3\sqrt{2}/4\right) a\omega^2 \text{ sech } (\pi\omega/2). \tag{8}$$

Now the region of instability is shifted towards higher frequencies due to the factor ω^2. The most important difference, compared with the ordinary Duffing oscillator, is the independence of the condition (8) of the damping constant Γ. Both above conditions are necessary, but not sufficient, for the full chaos to occur. The threshold of the positive Lyapunov exponent lies at the forcing parameters f_0 and a somewhat greater [10,11] than those implied by the conditions (7) and (8).

When the assumption of a weak effective damping $\Gamma = T/c$ (very light or very stiff substrate) underlying the conditions (7) and (8) is not fulfilled, we use numerically obtained time series to determine the regions of chaos. In the next section we also show examples of harmonics and subharmonics generation efficiencies, of reflection coefficients, and of an analogue of the local density of states in a large range of the model parameters so as to compare the behaviour of the system in the regular and in the chaotic regimes.

3 Physical characteristics of the nonlinear surface response

To get the time-series needed to characterise the response of the surface atom for arbitrary values of the model parameters we solved equations (2) and (6) with the use of a simplectic integrator based on the Verlet algorithm and on a step adaptive Runge- Kutta-Fehlberg method [12]. This method allowed us to obtain stable solutions of sufficient lengths so as to obtain reliable frequency spectra of the corresponding time series as well as satisfactory estimates for the Lyapunov exponent.

In the case of the system with the external applied force $f_0(t) = f_0(\omega)\cos(\omega t)$ (Eq. (2)) the quantity of interest is the efficiency of generation of harmonics and subharmonics. The efficiency E_n is defined as the ratio $E_n = u(n\omega)/f_0(\omega)$, where $u(n\omega)$ is the nth Fourier component of the displacement $u(t)$ satisfying equation (2). Integer values of index n correspond to harmonics and fractional values to subharmonics. Analogous quantities relevant in the phonon scattering experiment are reflection coefficients for particular harmonics $R_n = u_r(n\omega)/a$ defined as the ratio of the nth Fourier component of the reflected wave to the incident amplitude a. In the present model the reflected wave $u_r(t)$ is deduced from equation (6). The quantity R_1 is the ordinary reflection coefficient considered in models of harmonic surfaces [7].

For comparison with the detailed analysis existing for the Duffing oscillator we chose the coefficients of the local anharmonic potential after reference [13]: $M = 1$, $A = -10$, $B = 100$, $C = 0$, $T/c = 1$ and the frequency ω of the applied force $f_0(t) = f_0(\omega)\cos(\omega t)$ equal to $\omega = 3.5$. Figure 1 shows the efficiencies of generation of the lowest harmonics and subharmonics as well as the lowest reflection coefficients. In the upper part of Figure 1 the Lyapunov exponent is represented to indicate the regions of chaos which correspond to $\lambda > 0$ [14]. The present values for the Lyapunov exponent are consistent with the results of reference [13]. The comparison of r.h.s. of equations (2) and (6) makes clear that $E_n = R_n \times c/2T\omega$ for $n \neq 1$. The higher harmonics and subharmonics, except for $n = 1$, vanish in the limit $a \to 0$ and $f_0 \to 0$ in which case the harmonic approximation is valid. With increasing the applied force f_0 and the incident amplitude a the second harmonic $n = 2$ shows up progressively. A significant third harmonic $n = 3$ appears in the region of a fast rise of the fundamental efficiency E_1. A visible point of recession in the fundamental efficiency and of a step-like decrease in the reflection coefficient R_1 for $f_0 \approx 0.6$ is related with generation of harmonics $n > 3$ not shown in Figure 1.

The onset of chaos at $a = 0.1184\ldots$ or $f_0 = 0.8288\ldots$ is preceded by the appearance of the second subharmonic $n = 1/2$ which is equivalent to the doubling of the period of the solution of equations (2) and (6) with respect to the period of the perturbation $2\pi/\omega$. The detailed behaviour of the subharmonics in this region is shown in Figure 2. One can see a consecutive appearance of subharmonics $1/2$ and $1/4$ which is characteristic for the Feigenbaum scenario of the chaos onset. It is interesting that the subharmonic $1/8$ is rather weak. The multiplication of the period by 8 is, nevertheless, clear and is realised by simultaneous appearance of subharmonics $3/8$ and $5/8$. A part of the sequence of period doublings is presented in Figure 3 by the corresponding phase portraits. The values

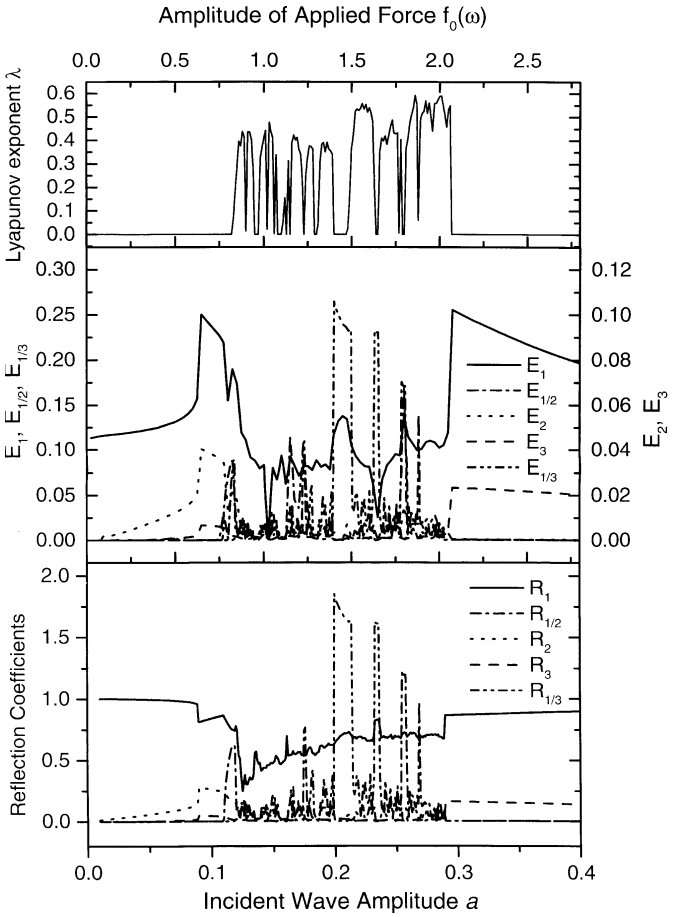

Fig. 1. Generation efficiencies E_n of the lowest harmonics and subharmonics by the external oscillatory force $f(t) = f_0(\omega)\cos(\omega t)$ applied to the surface atom in the potential $V_0(u) = -5u^2 + 25u^4$ and the reflection coefficients R_n, for the incident wave $u(ct + x) = a\sin(\omega t + x\,\omega/c)$; $\omega = 3.5$, $T/c = 1$. The upper part shows the corresponding Lyapunov exponent.

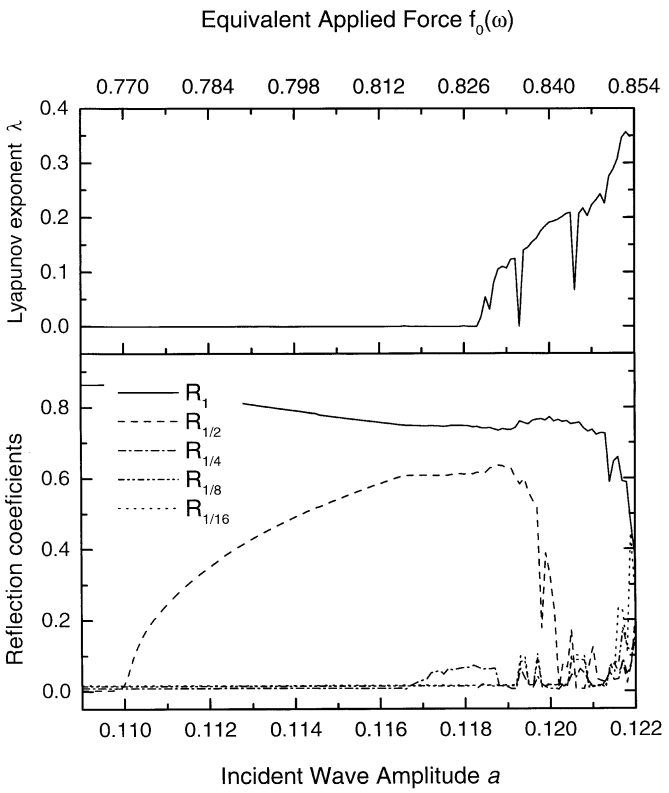

Fig. 2. The lowest harmonics and the Lyapunov exponent near the onset of chaos in the system from Figure 1.

of the incident amplitudes corresponding to the first three period doublings are: $a_1 = 0.110$, $a_2 = 0.1167$, $a_3 = 0.1181$, which give two estimates for the constant δ in the Feigenbaum formula $a_{ch} - a_m \propto \delta^{-m}$: $\delta = 4.941$ and $\delta = 5.667$. The latter values are close to the universal value $\delta = 4.6692...$ [14].

The region of chaos, corresponding to the positive Lyapunov exponent $\lambda > 0$, interrupted by windows of periodic motion ($\lambda = 0$) extends from $a = 0.1184\ldots(f_0 = 0.8288\ldots)$ to $a = 0.2863\ldots(f_0 = 2.0041\ldots)$. The reflected wave differs markedly in cases of periodic and of chaotic motion of the surface. The periodic motion shows a discrete frequency spectrum consisting of odd harmonics of a certain subharmonic of the incident frequency ω [9]. The spectra in the chaotic regions are irregular and continuous with narrower or broader maxima corresponding to the frequencies present in the neighbouring periodic windows. A comparison of spectra in a window of periodicity equal to $7 \times 2\pi/\omega\,(a = 0.137)$ and in the adjacent region of chaos ($a = 0.141$) is exhibited in Figure 4. A closer insight into the power spectra of the chaotic solutions shows that they tend to constant non-zero values for $\omega \to 0$ which behaviour witnesses to a lack of long-time correlations [15].

The largest window of periodicity close to $a = 0.200$ ($f_0 = 1.4$) is associated with a strong third subharmonic, see Figure 1. Figure 5 shows the corresponding frequency spectrum. The consecutive odd harmonics are very well fitted by an exponential function. Figures 6a and 6b exhibit a comparison of the phase portraits in the regular window $a = 0.200$ and in the neighbouring region of chaos $a = 0.225$, which allows one to appreciate the character of the chaotic motion. The basic shape corresponding to the period triplication is repeated with some unexpected distortions of a dephasing character. This is the cause that traces of the broadened subharmonic 1/3 and its odd harmonics are present in the chaotic spectrum in analogy to the subharmonic 1/7 in Figure 4. Generally, this behaviour is characteristic of unstable periodic orbits [9]. Beyond the upper limit of chaos $a = 0.288\ldots(f_0 = 2.016\ldots)$ the motion becomes periodic with the periodicity corresponding to the incident frequency and with only odd harmonics. The latter property results from a particular choice of a symetric surface potential.

To delimit the region of chaos for different values of the frequency of the incident wave Figure 7 shows the Lyapunov exponent as a function of ω for some selected incident amplitudes.

Anharmonicity modifies the shape of the surface resonance. To visualise this we define the energy loss

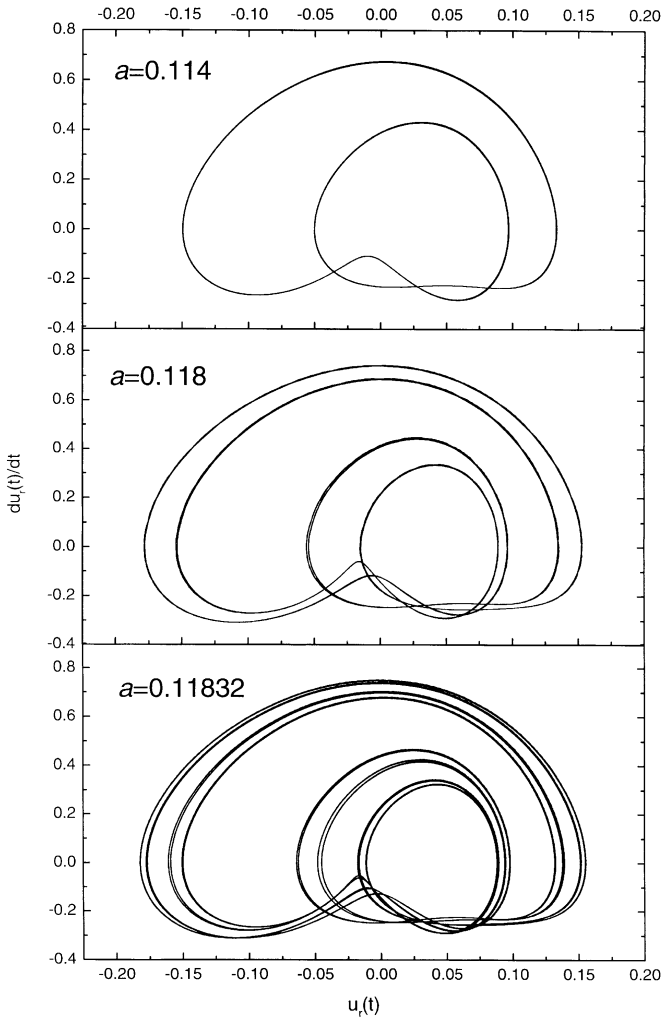

Fig. 3. Phase portraits of the motion of the surface atom under the incident wave near the onset of chaos in the system of Figure 1. Visible is doubled, quadrupled and octupled period.

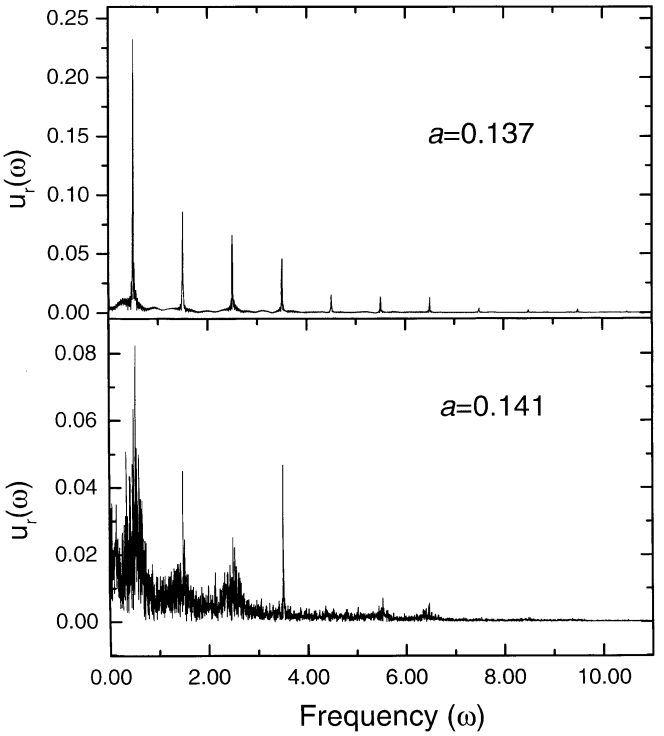

Fig. 4. Fourier transforms $u_r(\omega)$ in a window of periodic motion (amplitude of the incident wave $a = 0.137$) and in the neighbouring chaotic region ($a = 0.141$). Visible is the subharmonic 1/7 with its odd harmonics.

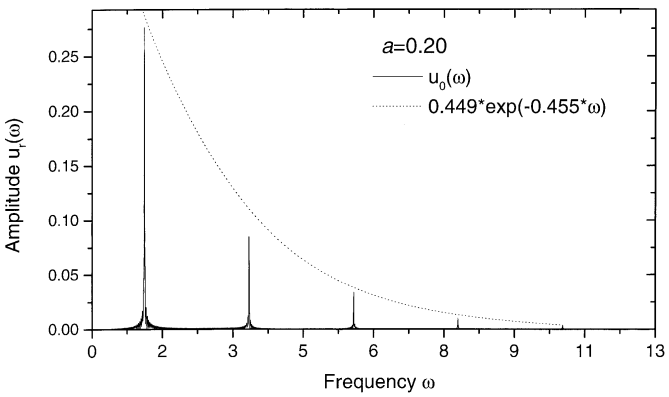

Fig. 5. Fourier transform $u_r(\omega)$ in the largest periodic window corresponding to the period triplication. The intensities of the consecutive odd harmonics are well approximated by an exponential function.

coefficient as the power transmitted to the system per square of the amplitude of the applied force. The energy loss coefficient then describes the relative decrease in the intensity of the initial radiation beam due to the inelastic scattering. In the limit of weak amplitudes this quantity is equivalent to the local density of states LDOS. Figure 8 shows the evolution of the energy loss coefficient with increasing amplitude $f_0(\omega)$. One can see an initial Lorenzian shape, its broadening, its shift towards lower frequencies and its final break down associated with the onset of chaos. A behaviour of the kind shown in Figure 8 is expected in experiments with inelastic scattering of a radiation sent from outside of the crystal from the anharmonic surface [16].

4 Resonant desorption of the surface atom

When the amplitude of the applied external force or of the incident wave is weak enough the motion of the surface atom rests confined in the neighbourhood of one of the two minima of the potential given by equation (5). With increasing amplitude of the perturbation the motion becomes strongly anharmonic and often chaotic. For still slightly greater amplitude the atom eventually starts to visit the second minimum. It should be stressed that the chaos usually occurs earlier than the transition to the second minimum. This transition is a model of desorption. For realistic cases different values of the coefficients A, B and C of

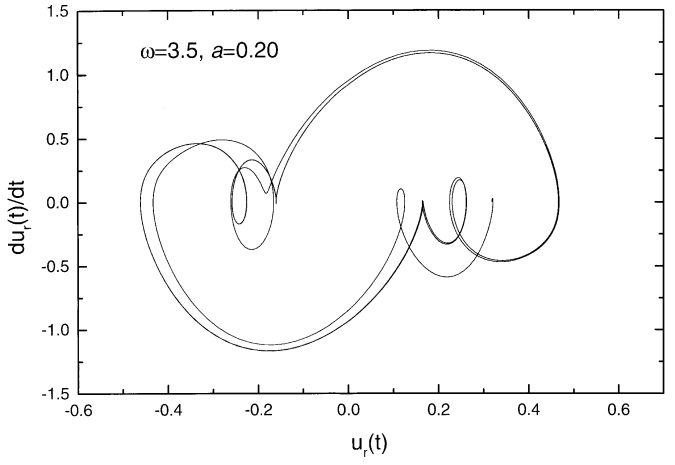

(a)

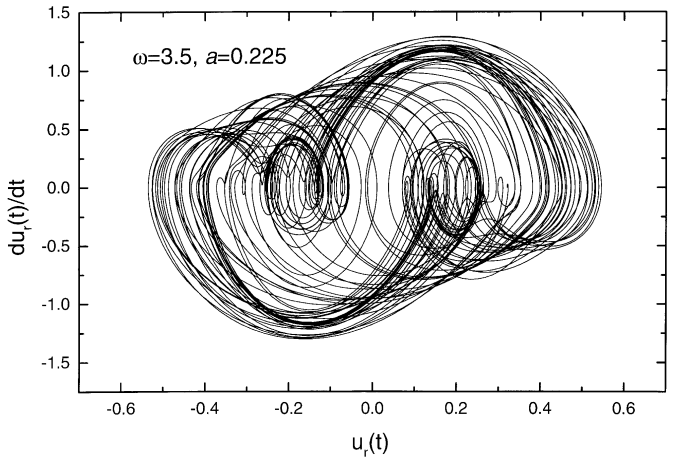

(b)

Fig. 6. Comparison of the phase portraits in (a) the window of periodic motion (amplitude of the incident wave $a = 0.20$), and (b) the neighbouring region of chaotic motion ($a = 0.225$).

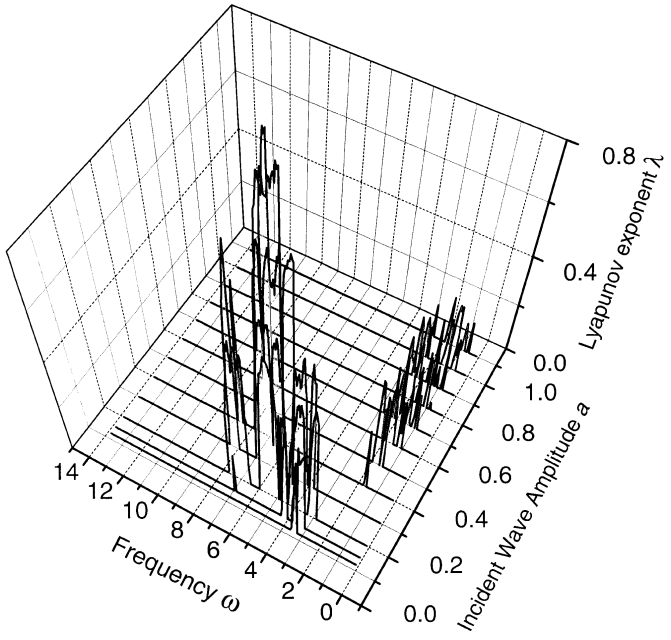

Fig. 7. Lyapunov exponent as a function of the frequency and amplitude of the incident wave in the scattering of phonon from the surface of Figure 1.

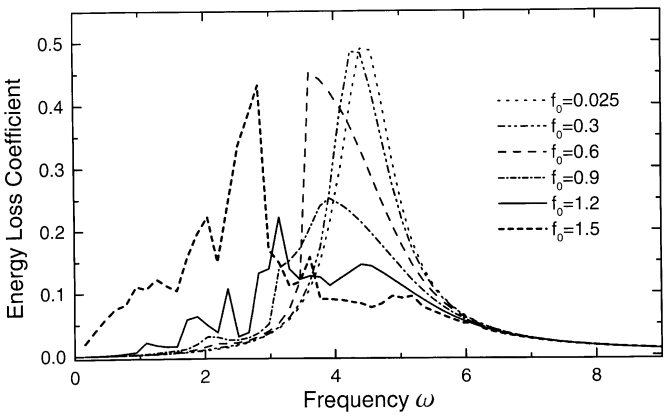

Fig. 8. Energy Loss Coefficient, *i.e.* the power transmitted to the system per squared amplitude of the applied force (equivalent to LDOS for weak amplitudes) as a function of frequency in the region of a surface resonance for various values of the applied amplitude. The model parameters same as in Figure 1.

equation (5) should be studied as well as different forms of the potential so as to correctly model the interaction of the atom with the surface at long distances [3,17].

Here we have studied the phenomenon for the same values $A = -10$, $B = 100$, $C = 0$ as used in previous section in order to give a complete set of data for this case. Figure 9 shows the minimal external force $f_0(\omega)$ capable of driving the surface atom out the initial minimum within the time $t = 4 \times 10^2$ in the units of the model. The desorption is particularly enhanced for a frequency slightly lower than the resonance frequency of the harmonic part of the potential $\omega_r = \sqrt{2A/M}$. Side minima in the curve occur close to the harmonics and subharmonics of the resonance frequency especially for low values of the effective damping T/c. This effect can be called resonant desorption. The present numerical results are in qualitative agreement with approximate calculations done for similar system by Reichl and Zheng [18] in the frequency range $\omega_r < \omega < 2.0\omega_r$.

An analogous set of curves for the desorption induced by a wave coming from the bulk is shown in Figure 10. Generally, the enhancement of the desorption at the resonant frequency as well as at its subharmonics and harmonics is very similar. The main difference in the behaviour concerns the limits $\omega \to 0$ and $\omega \to \infty$. The minimal amplitude capable of driving the atom out of its initial minimum tends to infinity for small frequencies and shows a behaviour $a \sim f_{0\,\min}/\omega$ for large frequencies.

The described features are particularly pronounced for small effective damping $T/c = \sqrt{\rho/T}$ which means that the resonant character of the desorption should be expected in relatively light and stiff substrates.

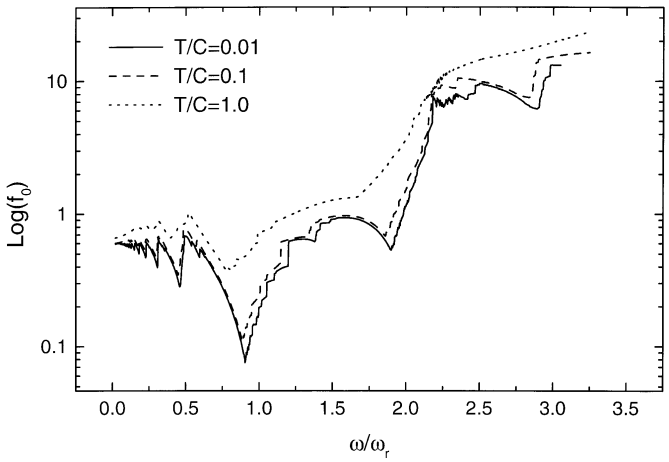

Fig. 9. Minimal external force f_0 capable of driving the surface atom from the initial potential minimum within time 4×10^2 for three different substrates.

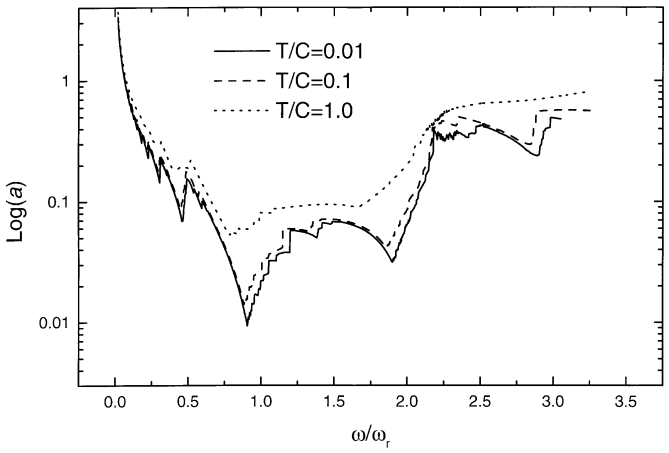

Fig. 10. Minimal amplitude a of the incident wave capable of driving the surface atom from the initial potential minimum within time 4×10^2. All parameters same as in Figure 9.

5 Discussion

The comparative study of the dynamics of the surface atom on a dispersionless substrate, subject to two kinds of perturbations: i) an oscillatory external force and ii) a monochromatic incident phonon coming from the bulk, reveals some analogies but also some differences. From the mathematical point of view the case i) is equivalent to the well known Duffing oscillator (Eq. (2)) whereas the case ii) involves a differential equation whose source term is a function of the incident wave (Eq. (6)). In both cases an increase in the amplitude of the perturbation engenders the second and, further, higher harmonics. Still larger amplitudes result in a sequence of period doublings, which eventually ends up with the onset of chaos according to the Feigenbaum scheme. In turn, an interval of amplitudes appears, which is marked by a chaotic response interrupted by windows of periodic motion. Above a certain value of the amplitude the chaos gives way to a periodic motion with the period equal to the period of the perturbation and with only odd harmonics. The latter property results from the specific choice of the symmetric surface potential. Generally, the scheme of appearance and destabilisation of periodic orbits is fulfilled [9].

The escape of the surface atom out of its initial equilibrium location is a simple model of desorption in the given surface potential. Physisorbed neutral atoms are expected to better obey the present model because chemisorption and ionisation involve electronic degrees of freedom, here only accounted for through phenomenological coefficients of the surface potential. The energetic barriers related to chemisorption are usually much higher than the range of phonon energies [17,19]. Resting within the present model one can notice an enhancement of the desorption for a resonance frequency and, to a smaller extent, for its harmonics and subharmonics. The frequency of the resonant desorption is slightly lower than the frequency of the surface resonance in the harmonic approximation. The present resonant desorption is a classical analogue of the quantum evaporation [20]. Whereas the quantum desorption requires the frequency of the perturbation corresponding to the quantum level with respect to the desorbed state, the present enhanced desorption is related to the classical resonance frequency.

The calculations shown in Sections 3 and 4 do not involve quantum effects so that they are expected to describe atoms which are heavy enough and at sufficiently high temperatures. The study of effects of thermal fluctuations and of finite coherence lengths of the perturbations concomitant in such circumstances, are now under progress and will be presented in future.

Computational methods used in this work and developed by Z. Łodziana have been supported by the grant 2-PO3B 004 14 of Committee for Scientific Research (Poland). Valuable remarks of Prof. W. Gadzuk, Dr L. Dobrzyński and Dr M. Lefranc are thankfully acknowledged.

References

1. G. Benedek, in *Nonequilibrium Phonon Dynamics*, edited by W.E. Bron (Plenum, New York, 1985), p. 601.
2. For a review see *e.g.* P. Zieliński, Acta Phys. Pol. **89**, 251 (1996).
3. S. Holloway, in *Interaction of Atoms and Molecules with Solid Surfaces*, edited by V. Bortolani, N.H. March, M.P. Tosi (Plenum, New York, 1980), p. 567.
4. P. Zieliński, Z. Łodziana, T. Srokowski, Prog. Surf. Sci. **59**, 265 (1998); *ibid.*, Physica B **263-264**, 719 (1999).
5. G. Duffing, *Erzwungene Schwingungen bei veränderlicher Eigenfrequenz* (Vieweg, Braunschweig, 1918); for discussion of chaotic properties see *e.g.* J.M.T. Thompson, H.B. Stewart, *Nonlinear Dynamics and Chaos - Geometrical Methods for Engeneers and Scientists* (Wiley, Chichester, 1986), p. 3.
6. See for example: N.H. Fletcher, T.D. Rossing, *The Physics of Musical Instruments* (Springer-Verlag, Berlin, 1991), p. 39; for mathematical bases see: A.V. Bitsadze,

Urovnienyia Matematicheskoy Fiziki (Nauka, Moskva, 1976), p. 163.
7. P. Zieliński, L. Dobrzyński, B. Djafari-Rouhani, Z. Phys. B **104**, 299 (1997).
8. A.H. Nayfeh, D.T. Mook, *Nonlinear Oscillations* (Wiley-Interscience, 1979).
9. R. Gilmore, J.W.L. McCallen, Phys. Rev. E **51**, 935 (1995).
10. E.W. Jacobs, A.R. Bulsara, W.C. Schieve, Physica D **34**, 439 (1989).
11. A.J. Lichtenberg, M.A. Lieberman, *Regular and Chaotic Dynamics* (Springer-Verlag, New York, 1992), p. 560ff.
12. D.J. Isbister, D.J. Searles, D.J. Evans, Physica A **240**, 105 (1997).
13. W.-H. Steeb, W. Erig, A. Kunick, Phys. Lett. A **93**, 267 (1983).
14. H.G. Schuster, *Deterministic Chaos - An Introduction* (VCH, Weinheim, 1988), p. 52.
15. T. Geisel, A. Zacherl, G. Radons, Phys. Rev. Lett. **59**, 2503 (1987); *ibid.*, Z. Phys. B **71**, 117 (1988).
16. H. Ibach, Surf. Sci. **299/300**, 116 (1994); G. Benedek, P.J. Toennies, *ibid.*, 578 (1994).
17. P. Feulner, D. Menzel, *Laser spectroscopy and photochemistry on metal surfaces* (Word Scientific, Singapore, 1995).
18. L.E. Reichl, W.M. Zheng, Phys. Rev. A **29**, 2186 (1984).
19. See for example: J.W. Gadzuk, Phys. Rev. Lett. **76**, 4234 (1996); D. Bejan, thesis University of Paris Sud, 1998, and references given therein.
20. M. Brown, A.F.G. Wyatt, J. Phys.-Cond. Matter **2**, 5025 (1990); A.F.G. Wyatt, Nature **391**, 56 (1998).